Penning ionization electron spectroscopy of organic molecules: stereochemistry of molecular orbitals

Yoshiya Harada

Department of Chemistry, College of Arts and Sciences, The University of Tokyo, Komaba, Meguro, Tokyo 153, Japan

Abstract – In Penning ionization electron spectroscopy, the kinetic energy of electrons ejected by collisions between targets (gas or solid) and metastable atoms is analyzed. In a gas phase spectrum, an orbital exposed outside the repulsive molecular surface gives a stronger band than does an inner orbital localized inside the surface. Thus, the relative band intensity of the spectrum depends on the spatial electron distribution of *individual* molecular orbitals. Furthermore, with the introduction of a bulky group some molecular orbitals can be protected from the impact of metastable atoms and become less reactive to the metastables. Therefore, the analysis of the relative band intensity also provides information on the steric shielding effect on the molecular orbital. When Penning ionization electron spectroscopy is applied to the solid, the electron distribution of individual molecular orbitals exposed outside the outermost surface layer is selectively probed. In this case, we can see the shape of the molecular orbital from various directions, if we can control the orientation of surface molecules. The characteristics of Penning ionization electron spectroscopy stated above have been applied to the study of stereochemical properties of various organic molecules.
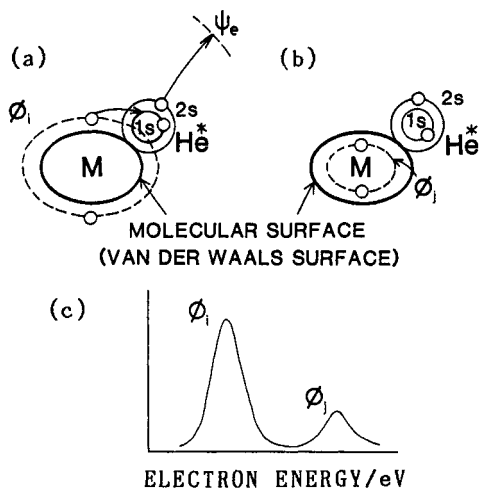
INTRODUCTION

Fig. 1. Schematic diagram showing the relation between the distribution of the molecular orbital and the intensity of the corresponding band.

Various intermolecular processes including chemical reactions start with effective overlapping of the tails of molecular wave functions. To elucidate these processes, therefore, one needs information on the stereochemistry of *individual* molecular orbitals, especially their spatial electron distributions in the frontier region near the molecular surface. Recent studies (ref. 1, 2) have shown that such information can be obtained by Penning ionization electron spectroscopy (ref. 3, 4), in which the kinetic energy of electrons ejected by collisions between targets T and metastable atoms A* is analyzed:

$$T + A^* \rightarrow T^+ + A + e^-, \qquad (1)$$
$$e^- \text{ for energy analysis.}$$
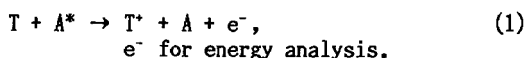
Usually metastable rare gas atoms such as He*(1s2s,2^1S,20.62 eV), He*(1s2s,2^3S,19.82 eV), and Ne*($2p^5$3s,$^3P_2$,16.62 eV) are used as A*.

Figure 1a shows the Penning ionization process due to the collision between a molecule M and a metastable helium atom. As shown in the figure, an electron in an orbital of M, ϕ_i, transfers to the 1s hole of He* and its 2s electron is ejected to an orbital of the continuam state, ψ_e. The transition probability Γ of this process is given by (ref. 5)

$$\Gamma \propto | < \phi_i(1) \chi_{2s}(2) | 1/r_{12} | \chi_{1s}(1) \psi_e(2) > |^2. \qquad (2)$$

Therefore, the relative intensity of the bands in a Penning ionization electron spectrum (PIES) largely depends on the overlapping of the relevant orbital ϕ_i and the 1s orbital of He* . Since the metastable atom can approach up to the repulsive surface of the molecule, which can be estimated from the van der Waals (VDW) radii of the atoms in the molecule, the degree of overlap of ϕ_i and χ_{1s} is essentially determined by the distribution of ϕ_i outside the repulsive molecular surface (VDW surface) (ref. 6). Thus,

3a₁   1e

3a₁   NH₃   He* PIES

1e

10   8   6   4   2   0
3a₁   PIES Electron Energy/eV

NH₃   1e   Hel UPS

10   8   6   4   2   0
UPS Electron Energy/eV

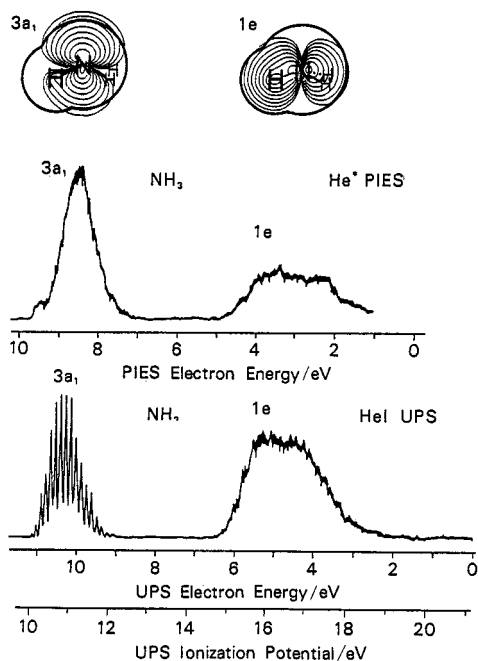10   12   14   16   18   20
UPS Ionization Potential/eV

Fig. 2. He*(2³S) PIES and He I UPS for
ammonia and the electron density maps
for the relevant orbitals. The thick
solid curves in the maps indicate the
molecular surface.

an outer orbital "exposed" outside the VDW
surface of the molecule gives a larger Γ
value and, hence, a stronger band in PIES (Fig.
1a and c) than an inner orbital localized
inside the surface (Fig. 1b and c).

Let us consider an example of the ammonia
molecule (ref. 6). Figure 2 shows the He*(2³S)
PIES and He I (21.22 eV) ultraviolet photo-
electron spectrum (UPS). As is seen from the
figure, in the PIES the first band due to the
lone pair orbital is enhanced relative to the
second band due to the NH bonding orbitals.
This can be explained by the electron density
maps shown at the top of Fig. 2; the lone pair
orbital extended outside the VDW surface
(indicated by thick curves in the maps) of the
molecule easily interacts with He* metastables
and gives a stronger band in PIES, while the
bonding orbitals localized inside the VDW
surface give a weaker band.

PIES OF MOLECULES

The features of the molecular PIES mentioned
above was applied to the study of the stereo-
chemical properties of various molecular
orbitals as well as to the assignment of the
UPS bands in a large number of molecules (ref.
1, 2). Some examples will be shown below.

Figure 3 shows the PIES and UPS of benzene
(ref. 6, 7). A theoretical PIES (see below)
and the electron density map for each molec-
ular orbital obtained by the *ab initio* MO method with a 4-31G basis set are also shown. In
the PIES the π (e₁ₛ and a₂ᵤ) bands are seen to be stronger than the σ bands. This can
be understood easily, because the π orbitals extending out of the molecular plane
interact with metastable atoms more effectively than the σ orbitals. The electron
density maps in Fig. 3 well explain this spectral feature. Furthermore, among the σ
orbitals, the a₁ₛ orbital gives a relatively strong band in the PIES, because it has CH
bonding character and is distributed outside the molecule. On the other hand, the b₂ᵤ

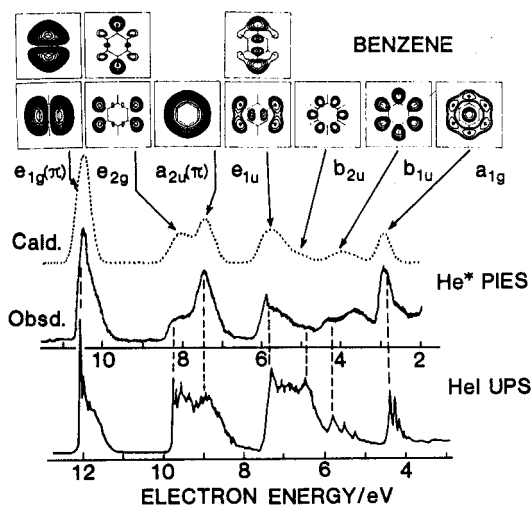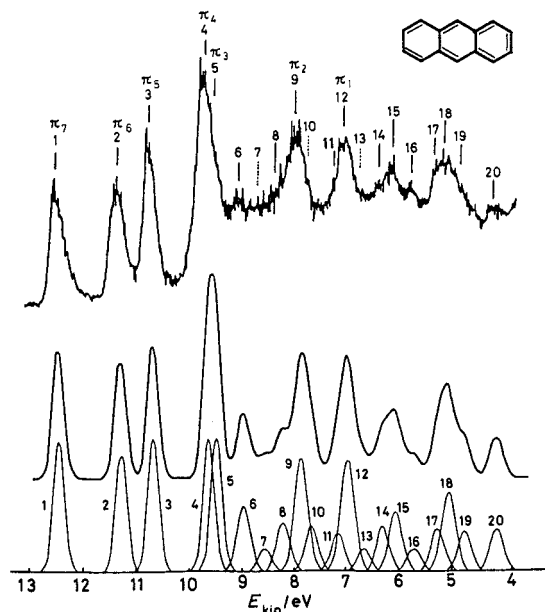
BENZENE

e₁g(π)   e₂g   a₂ᵤ(π)   e₁ᵤ   b₂ᵤ   b₁ᵤ   a₁g

Cald.

Obsd.

10   8   6   4   2

He* PIES

Hel UPS

12   10   8   6   4
ELECTRON ENERGY/eV

Fig. 3. Theoretical PIES (upper), He*(2³S)
PIES (middle), and He I UPS (lower) of
benzene together with the electron den-
sity maps for the relevant orbitals. The
maps are drawn for a plane 1.7 Å above
the molecular plane.

13   12   11   10   9   8   7   6   5   4
E_kin/eV

Fig. 4. He*(2³S) PIES (upper) and theoretical
PIES (lower) of anthracene.

band is almost missing in the PIES, although the corresponding band has appreciable intensity in the PIES. This is ascribed to the distribution of the b_{2u} orbital localized along the carbon skeleton (see the electron density map) and shielded by the π orbitals. As was described above, the relative intensity of the PIES band can be estimated from the distribution of molecular orbitals outside the repulsive molecular surface (VDW surface). Hence, we have defined the exterior electron density (EED) for each MO ϕ_i by (ref. 7)

$$(EED) = \int_\Omega | \phi_i(r) |^2 dr, \tag{3}$$

where the integration is taken over the region Ω outside the VDW surface of the molecule. The theoretical PIES in Fig. 3 was synthesized from Gaussiasn-type bands with area proportional to the respective EED's and is seen to be in good agreement with the observed PIES.
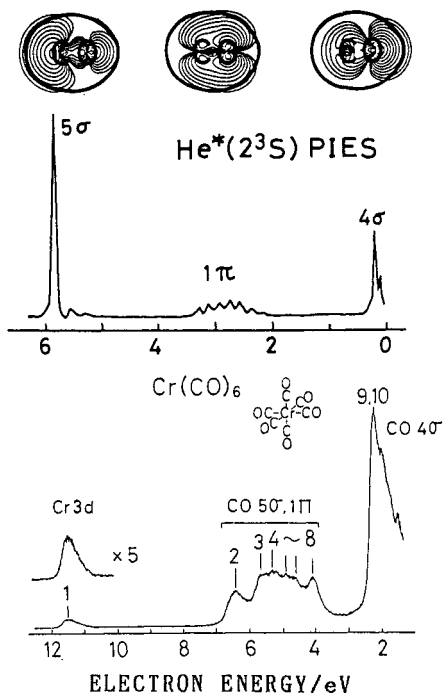
Figure 4 shows the observed and theoretical PIES of anthracene (ref. 8). As is seen in the figure, the theoretical PIES well reproduces the relative intensity of the observed bands. Thus, the EED analysis allows us to assign all the bands in the He I UPS, where only the highest five π bands have been assigned previouly.

With the introduction of a bulky group some orbitals can be protected from the impact of metastable atoms and become less reactive in Penning ionization. Such a steric shielding effect has been found in the PIES of organometallic complexes (ref. 9) and also of some substituted anilines (ref. 10) and nitriles (ref. 11). Figure 5 shows the PIES of carbon monooxide (ref. 9) and chromium hexacarbonyl (ref.12). In the case of CO the first band is enhanced relative to the other bands, because the corresponding 5σ orbital protrudes largely outside the molecular surface. In the PIES of Cr(CO)$_6$ band 1 due to Cr 3d orbitals is much weaker than the other bands, since the Cr atom is surrounded by six CO molecules and, hence, the electrons in the atom cannot interact effectively with metastables. On the other hand, bands 9 and 10 related to the 4σ orbital of CO is much enhanced in comprison with bands 2 to 8 originated from the 5σ and 1π. This is ascribed to the character of the 4σ orbital, which has large electron density on the oxygen atom (see the top of the figure). Thus, orbitals of Cr(CO)$_6$, predominantly 4σ in character, are exposed in the outermost region of the molecule.

Fig. 5. He*(2³S) PIES of carbon monooxide and chromium hexacarbonyl.

In contrast to the case of Cr(CO)$_6$, the Cr 3d orbitals of dibenzenene chromium are not well shielded by the benzene rings (ref. 12). As shown in Fig. 6, bands 1 and 2 in the PIES due to the Cr 3d orbitals are relat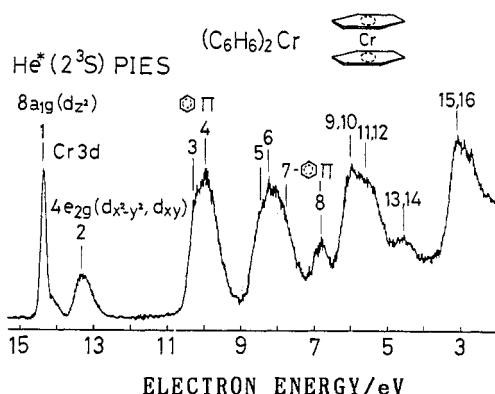ively strong. In particular, band 1 originated from the Cr 3d$_{z^2}$ orbital is stronger than a π band of the benzene ring; the intensity of band 1 is larger than a quarter of the integrated intensity of bands 3 and 4, which are related to four π orbitals. This shows that the Cr 3d$_{z^2}$ orbital is distributed outside the molecule, penetrating the planes of the benzene rings. Chromium hexacarbonyl and dibenzene chromium are model compounds for carbon monooxide and benzene adsorbed on a metal surface. It is interesting to note that our results are consistent with those observed in the PIES of metal surfaces; CO molecules adsorbed perpendicularly on a metal surface shield the metal d orbitals, while benzene molecules adsorbed flat on the surface do not (ref. 13).

Fig. 6. He*(2³S) PIES of dibenzene chromium.

Finally the study of hydrogen bonding by PIES will be described (ref. 14). When an intramolecular hydrogen bonding of the OH-X

type is formed in XCH_2CH_2OH molecules, the intensity of the n_x band is found to be much less than that of the corresponding n_x band in XCH_2CH_3 molecules. This is due to the fact that upon the formation of the hydrogen bonding the access of metastable atoms to the n_x orbital becomes difficult owing to the steric shielding effect of the OH group. In the case of N,N'-dimethylaminoethanol, the temperature dependence of the n_x band intensity, which is an average of the intensities for bonded and dissociated forms, was analyzed and the population of the bonded conformer (0.83 at 23 °C, 0.29 at 300 °C) and some thermodynamic data for the dissociation of the hydrogen bonding (ΔH = 1.25 kJ mol^{-1}, ΔS = 29 J K^{-1} mol^{-1}) were obtained.

PIES OF SOLID SURFACES

When PIES is employed for the study of a solid surface, the following two characteristics are displayed (ref. 1, 2, 15). Firstly, PIES probes the outermost surface layer of the solid surface selectively because metastable atoms do not penetrate into the inner layers. This is not the case in other electron spectroscopies such as photoelectron, Auger, and electron impact spectroscopies, where photons or electrons used for the excitation sources penetrate into the inner layers. Secondly, PIES enables us to study the electron distribution of individual orbitals in the exterior region outside the solid surface. In gas-phase molecules, which are randomly oriented with respect to the direction of the metastable beam, the relative intensity of the PIES bands reflects the overall spread of individual orbitals. On the other hand, the PIES of the solid surface provides information on the wave function tails of individual orbitals at a definite molecular part exposed outside the surface. This character of surface PIES can be used to probe the geometrical orientation of surface molecules.

Figure 7 shows an example of benzene layers adsorbed on a graphite cleavage plane at 130 K (ref. 16). The spectrum (a) was measured for a clean graphite substrate and spectrum (b), (c), and (d) were obtained from substrates exposed to benzene vapor of 5 ×10^{-7} Torr for 10, 100, and 400 s, respectively. The thicknesses of the adsorbed layers were estimated to be a few monolayers at a 10 s exposure and more than several tens of monolayers at a 400 s exposure. In Fig. 7 (a) the relative intensities of the π bands are much stronger and those of the σ bands are much weaker compared to the case of the gas-phase PIES in Fig. 3. This is accounted for, if we assume that the benzene molecules are oriented flat to the substrate. As can be seen from Fig. 8 (a), if a metastable atom approaches a benzene molecule oriented parallel to the graphite cleavage plane, a π orbital exposed outside the surface should interact effectively with the metastable atom and give a strong band in the PIES, while a σ orbital shielded by the π should give a weak band. When the surface molecule is tilted on the substrate, the σ bands are expected to become stronger in the spectrum, because the σ orbitals are also exposed outside (Fig. 8(b)). In fact, the intensity of the σ bands gradually increases with increasing exposure time (see Fig. 7 (b) to (c)), showing that molecules at the outermost layer gradually become tilted with increasing film thickness.
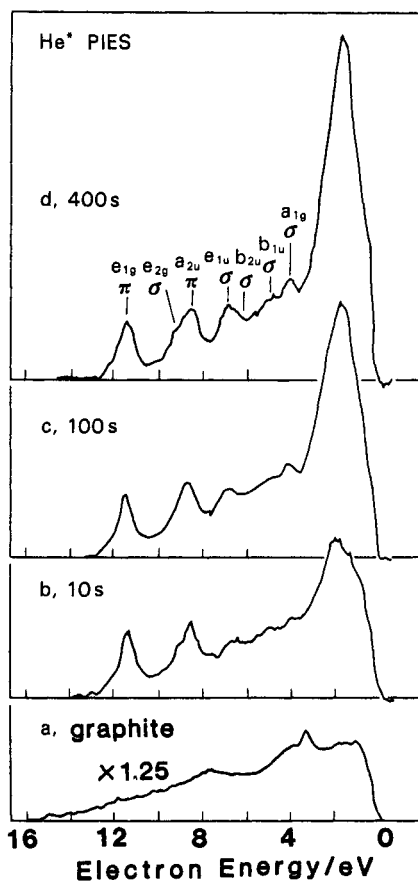

Fig. 7. He*(2^3S) PIES of benzene adsorbed on a graphite cleavage plane. (a) Clean graphite, (b) exposed to benzene vapor (5 × 10^{-7} Torr) for 10 s, (c) 100 s and (d) 400 s.

Figure 9 shows the PIES of two kinds of iron phthalocianine (FePc) films (ref. 17). Film A is a monolayer prepared by vacuum sublimation onto a graphite substrate held at 213 K. Film B is a crystalline one deposited on a stainless steel substrate at room temperature. As illustrated on the right of the figure, molecules are arranged flat to the substrate in film A and are tilted in film B. In the flat molecular orientation, π-type orbitals extending normal to the molecular plane (xy plane) effectively interact with metastables, whereas σ orbitals distributed within the molecular plane and shielded by the π-type orbitals scarcely interact with metastables. Among the π-type orbitals, those mainly originated from the iron $3d_{yz}$, $3d_{zx}$, or $3d_{z^2}$ AO ($3d_\perp$-like MO) should interact with meta-
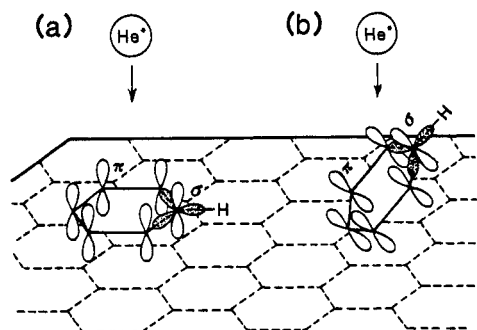
Fig. 8. Interaction between a metastable helium atom and a benzene molecule. (a) The molecule is oriented parallel to a graphite cleavage plane, (b) the molecule is tilted to the plane.
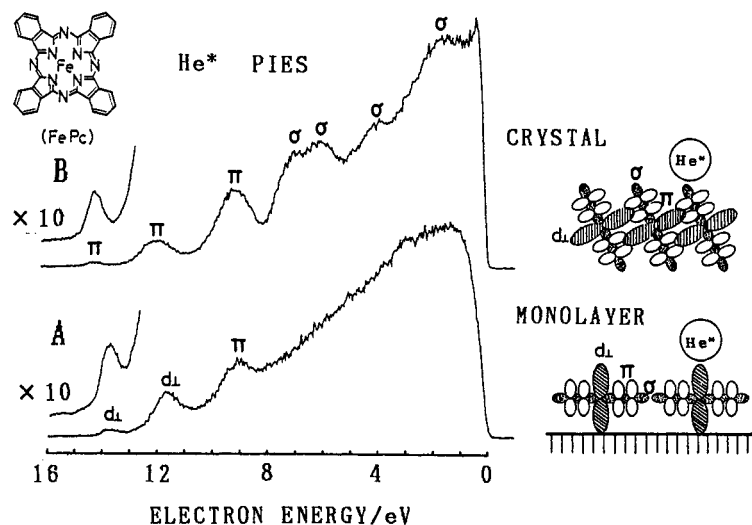
stables more effectively than those derived from the carbon and nitrogen $2p_z$ AO, because the former orbitals protrude outside the molecular surface more prominently than the latter ones. On the other hand, in the tilted molecular orientation, the σ orbitals as well as the π should be effectively attacked by metastables, but the $3d_\perp$-like orbitals with little distribution outside the film surface is expected to be scarcely attacked. As can be seen from Fig. 9, the relative intensity of the PIES bands for films A and B substanciate the above expectations regarding the ditributions of the surface orbitals.

Fig. 10 shows the PIES of two evaporated films (films I and II) of a long-chain alkane, tetratetracontane (n-$C_{44}H_{90}$) (ref. 18). Film I is a polycrystalline film prepared on a metal substrate at room temperature. Film II is a monolayer deposited on a graphite cleavage plane at low temperature (-60 °C). Since in the crystalline film (film I) molecules stand upright with their chains

Fig. 9. He*(2^3S) PIES of a monolayer film A and a crystalline film B of iron phthalocyanine (FePc). Films A and B were prepared by vacuum sublimation onto a graphite cleavage plane at 213 K and a stainless steel substrate at 298 K, respectively. The orientation of surface molecules in each film is illustrated on the right.
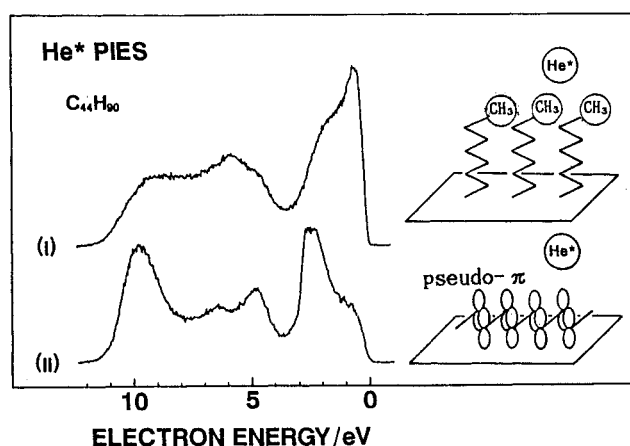

Fig. 10. He*(2^3S) PIES of evaporated films of tetratetracontane (n-$C_{44}H_{90}$) prepared on a metal (I) and a graphite substrate (II) together with the models of the molecular arrangements.

perpendicular to the substrate, metastable atoms effectively interact with the terminal methyl moieties (see the right part of Fig. 10). In fact, according to ab initio MO calculations, the features of the PIES are essentially due to molecular orbitals having a large distribution on the terminal methyl group. On the other hand, in the monolayer (film II) molecules lie flat on the substrate with their long chains parallel to the substrate plane. In this case, the features of the spectrum are due to molecular orbitals distributed on the side of the chain. For example, the peak located around 10 eV is originated from pseudo-π orbitals comprised of the C 2p and H 1s AO's and the peak at ca. 2.5 eV is attributed to orbitals due to the C 2s and H 1s AO's. The results shown here have been applied to the characterization of Langmuir-Blodgett (LB) films (ref. 18, 19). The LB films of cadmium stearate, for example, give almost the same PIES as that of Film I, which means that hydrocarbon chains of cadmium stearate stand upright exposing their methyl ends outside the film surface (ref. 18).

The examples shown in Figs. 9 and 10 indicate that surface PIES reflects the local distribution of individual orbitals at a definite molecular part exposed outside. If we can control the orientation of the surface molecules by means of the selections among various substrates, film preparation methods (vacuum deposition, adsorption, Langmuir-Blodgett technique etc.), deposition conditions (substrate temperature, deposition speed), and film treatments (e.g. annealing), we can probe the distribution of molecular orbitals from various direction and approach their "shape" or whole picture.

CONCLUDING REMARKS

We have shown that Penning ionization electron spectroscopy enables us to study the spatial electron distribution of individual molecular orbitals outside the molecular surface. From a chemical point of view, Penning ionization process is regarded as an electrophilic reaction of an excited atom A* with a molecule M; the reagent A* attacks an orbital of M and extracts an electron into the vacant orbital of A* yielding an ionic state of M$^+$. In this respect, the intensity of a band in PIES is connected with the reactivity of the corresponding orbital upon electrophilic attack by metastables. For solids, Penning spectroscopy probes the distribution of orbitals penetrated outside the outermost layer that essentially determines the properties of the solid surface. This unique feature of Penning spectroscopy should be further explored by its application to various solid surfaces.

REFERENCES

1. Y. Harada and H. Ozaki, Jpn. J. Appl. Phys. 26, 1201-1214 (1987).
2. K. Ohno and Y. Harada, Theoretical Models of Chemical Bonding, Part 3, ed. by Z. B. Maksić, Springer, Berlin, to be published.
3. V. Čermák, J. Chem. Phys. 44, 3781-3786 (1966).
4. A.J. Yencha, Electron Spectroscopy, Theory, Techniques and Applications, Vol.5, 197-373 ed. by C.R. Brundle and A.D. Baker, Academic, London (1984).
5. H. Hotop and A. Niehaus, Z. Phys. 228, 68-88 (1969).
6. K. Ohno, H. Mutoh and Y. Harada, J. Am. Chem. Soc. 105, 4555-4561 (1983).
7. K. Ohno, S. Matsumoto and Y. Harada, J. Chem. Phys. 81, 4447-4454 (1984).
8. T. Kajiwara, S. Masuda, K. Ohno and Y. Harada, J. Chem. Soc. Perkin Trans. II, 507-511 (1988).
9. Y. Harada, K. Ohno and H. Mutoh, J. Chem. Phys. 79, 3251-3255 (1983).
10. K. Ohno, S. Fujisawa, H. Mutoh and Y. Harada, J. Phys. Chem. 86, 440-441 (1982).
11. K. Ohno, S. Matsumoto, K. Imai and Y. Harada, J. Phys. Chem. 88, 206-209 (1984).
12. S. Masuda, M. Aoyama and Y. Harada, unpublished results.
13. W. Sesselmann, B. Woratschek, G. Ertl and J. Küppers, Surface Sci. 146, 17-42 (1984).
14. K. Ohno, K. Imai and Y. Harada, J. Am. Chem. Soc. 107, 8078-8082 (1985).
15. Y. Harada, Surface. Sci. 158, 455-472 (1985).
16. H. Kubota, T. Munakata, T. Hirooka, T. Kondow, K. Ohno and Y. Harada, Chem. Phys. 87, 399-403 (1984).
17. H. Ozaki and Y. Harada, J. Am. Chem. Soc. 109, 949-950 (1987).
18. Y. Harada, H.Hayashi, H. Ozaki, T. Kamada, J. Umemura, T. Takenaka, Langmuir, in press.
19. H. Ozaki, Y. Harada, K. Nishiyama and M. Fujihira, J. Am. Chem. Soc. 109, 950-951 (1980).